GLIA 37:19–30 (2002)

Oligodendrocytes Expressing Exclusively the DM20 Isoform of the Proteolipid Protein Gene: Myelination and Development

OLAF SPÖRKEL,[1] THOMAS USCHKUREIT,[1] HEINRICH BÜSSOW,[2] AND WILHELM STOFFEL[1]*
[1]*Laboratory of Molecular Neuroscience, University of Cologne, Cologne, Germany*
[2]*Institute of Anatomy, University of Bonn, Bonn, Germany*

KEY WORDS PLP/DM20 expression; $dm20_{only}$ knock-in mouse; myelin periodicity; myelin and oligodendrocyte degeneration

ABSTRACT Oligodendroglia and Schwann cells synthesize myelin-specific proteins and lipids for the assembly of the highly organized myelin membrane of the motor-sensory axons in the central (CNS) and peripheral nervous system (PNS), respectively, allowing rapid saltatory conduction. The isoforms of the main myelin proteins, the peripheral myelin basic isoproteins (MBP) and the integral proteolipid proteins, PLP and DM20, arise from alternative splicing. Activation of a cryptic splice site in exon III of plp leads to the deletion of 105 bp encoding the PLP-specific 35 amino acid residues within the cytosolic loop 3 of the four-transmembrane domain (TMD) integral membrane protein. To study the different proposed functions of DM20 during the development of oligodendrocytes and in myelination, we targeted the plp locus in embryonic stem cells by homologous recombination by a construct, which allows solely the expression of the DM20 specific exon III sequence. The resulting $dm20_{only}$ mouse line expresses exclusively DM20 isoprotein, which is functionally assembled into the membrane, forming a highly ordered and tightly compacted myelin sheath. The truncated cytosolic loop devoid of the PLP-specific 35 amino acid residues, including two thioester groups, had no impact on the periodicity of CNS myelin. In contrast to the PLP/DM20-deficient mouse, mutant CNS of $dm20_{only}$ mice showed no axonal swellings and neurodegeneration but a slow punctuated disintegration of the compact layers of the myelin sheath and a rare oligodendrocyte death developing with aging. *GLIA 37:19–30, 2002.*

INTRODUCTION

The major integral membrane protein constituents of the myelin sheath in the central nervous system (CNS) are the 30 kDa proteolipid protein (PLP) and the 26 kDa DM20 isoforms. Purification and protein sequencing established the primary structure of human and bovine PLP (Stoffel et al., 1983, 1985). The deletion of a 35 amino acid residue domain of the central part of PLP was first derived from protein analysis (Trifilieff et al., 1985) and later confirmed by cDNA sequencing (Nave et al., 1987). Comparison of the primary structure of PLP isoforms in different species indicated the strongly conserved amino acid sequence among mammalian species and the highly conserved positions of cysteine residues and of charged amino acids. These results further suggested a common tertiary structure of PLP isoforms throughout evolution from amphibian to man (Schließ and Stoffel, 1991).

Grant sponsor: the Deutsche Forschungsgemeinschaft; Grant number: SFB 243; Grant sponsor: Bundesministerium für Wissenschaft, Forschung und Technologie, in the Center of Molecular Medicine Cologne (ZMMK); Grant number: 01KS 9502.

*Correspondence to: Wilhelm Stoffel, Laboratory of Molecular Neurosciences, Institute of Biochemistry, Faculty of Medicine, University of Cologne, Joseph-Stelzmannstraße 52, D-50931 Cologne, Germany.
E-mail: wilhelm.stoffel@uni-koeln.de

Received 26 April 2001; Accepted 20 August 2001

DOI 10.1002/glia.10014

The polypeptide sequence of PLP led to the cloning and homology screening of the cDNA of several species (Milner et al., 1985; Schaich et al., 1986), the assignment of the *plp* locus to Xq23 (Willard and Riordan, 1985), and the elucidation of the *PLP* gene organization (Diehl et al., 1986). DM20 results from a 105 bp deletion by the activation of a cryptic splice site in exon III of the *PLP* gene, which was confirmed by the characterization of a DM20-specific cDNA (Nave et al., 1987).

Chemical studies revealed a four-transmembrane topology with the N- and C-termini located on the cytosolic side of the myelin membrane (Weimbs and Stoffel, 1994) in accordance with one of the hypothetical models (Popot et al., 1991). The PLP polypeptide is thioacylated by six long-chain fatty acids (palmitic, stearic, and oleic acid) at cysteine residues on the cytosolic side. This enhances the hydrophobicity of the PLP isoforms. The PLP-specific domain of cytosolic loop 3 missing in the DM20 isoform contains two of the six thioester groups (cys138 and 140) (Weimbs and Stoffel, 1992).

Several studies suggest that DM20 is the product of the genuine lipophilin gene (*plp*) and that the PLP-specific 105 bp were inserted during evolution because of an increasing function of PLP in mammalian myelin (Kitagawa et al., 1993; Yoshida and Colman, 1996). Different strategies have been applied to get insight into the poorly understood functions of the two PLP isoforms: analysis of point mutations in mouse, rat, and human (Nave et al., 1986; Boison and Stoffel, 1989; Yool et al., 2000), transgenic mice (Redhead et al., 1987; Johnson et al., 1995), and, most recently, null allelic mouse lines generated by gene targeting by homologous recombination (Boison and Stoffel, 1994; Boison et al., 1995; Klugmann et al., 1997; Stoffel et al., 1997; Uschkureit et al., 2000).

Recently, a gene targeting approach, a combined knock-in–recombinase approach, resulted in the generation of a mouse line exclusively expressing DM20 (Stecca et al., 2000). The analysis of this mutant suggested that DM20 is unable to replace PLP functionally in CNS myelin.

We used in the present study a different strategy of gene targeting, in which a replacement construct with exon III truncated by the 105 bp PLP-specific sequence was used for homologous recombination in embryonic stem cells to generate the exclusively DM20 expressing mouse line ($dm20_{only}$). Our results indicate that DM20 can functionally replace the PLP isoform with regard to myelin compaction (normal periodicity) and axon integrity. Despite minor morphological alterations of CNS myelin and oligodendrocytes, myelin and oligodendrocyte viability is maintain over the whole life span.

MATERIALS AND METHODS

Targeting Construct

The plasmid pDM20+neos used for the targeting experiments contains 4.2 and 1.6 kb of homologous sequences on the 5′ and 3′ site of the *loxP*-flanked neomycin-resistance gene, respectively. The *neo* gene was cloned in sense orientation into the *BamH*I site in intron III of the *plp* gene. The *thymidine kinase* gene (*TK*) was inserted at the 5′ end of the targeting construct. The two selection markers were under the control of the pgk promoter. The downstream 105 bp of exon III were deleted by splicing by overlapping extension PCR (SOE-PCR). The first PCR fragment was amplified with the primer II (exon II): 5′-GCTTGTTAGAGTGTTGTGCTAGATGTCTGG-3′ and $DM20^+$ as primer: 5′-AATCCTGAGGATGATCACCGTTGCGCTCAGGCCCTT-3′. The second fragment was amplified with primer $DM20^+$: 5′-AAGGGCCTGAGCGCAACGGTGATCATCCTCAGGATT-3′ and IVa (exon IV): 5′-CATACAACAGTCAGGGCATAGGTGATGC-3′. The DM20-specific sequence was obtained by PCR with the amplified fragments and the primer II and IVa.

Generation of Transgenic Mice

CJ7 ES cells were electroporated with the linearized targeting vector and ES cell clones carrying the targeted alteration of the *plp* gene were identified by Southern blot and PCR techniques. Two germline chimeras were obtained by injecting positive ES cells into C57/Bl6 blastocysts using standard methods (Bradley et al., 1984). Crossing heterozygous and hemizygous animals into the C57/Bl6 founder strain over seven generations led to a defined genetic background of the homozygous $dm20_{only}$ mouse line. Age-matched control littermates were compared with corresponding $dm20_{only}$ mice in all experiments.

Northern Blot Analysis

RNA of total brain (20 μg) of 16- to 20-day-old mice (Chomczynski and Sacchi, 1987) was separated by formaldehyde-agarose gel electrophoresis (1%), blotted to nitrocellulose (GeneScreen Plus; NEN Life Science Products, Boston, MA), and hybridized to a 1,362 bp randomly primed [^{32}P] *Pst*I fragment containing mixed cDNA sequences of the human and rat PLP cDNA sequence.

Quantitative RT-PCR

Total RNA was extracted from E12.5 to 55-day-old mouse tissue of brain, thymus, and heart; 10 μg RNA treated with RNAse-free DNAse were reverse-transcribed (SuperscriptII, Life Technologies, Karlsruhe, Germany). One-tenth of the mixture was used for each PCR in 50 μl in the presence of 0.1 μl [^{32}P]-dCTP. Samples were taken after 15, 17, 19, and 21 cycles and separated on 6% polyacrylamide gels. Gels were exposed to a PhosphorImager screen (Molecular Dynamics, Sunnyvale, CA) and analyzed with the ImageQuant software (Molecular Dynamics). The follow-

ing oligonucleotide primers were used. PLP-specific amplification: 5′ primer, 5′-ATCTGCGGCAAGGGC-CTGAGCGCAACCGTC-3′, 3′ primer, 5′-TAGTGTG-GCCGCAGCACCCACAAACGCAGC-3′; DM20-specific amplification: 5′ primer, 5′-ATCTGCGGCAAGGGC-CTGAGCGCAACGTTT-3′, 3′ primer, 5′-TAGTGTGG-CCGCAGCACCCACAAACGCAGC-3′; PLP and DM20: 5′ primer, 5′-CAAGCTCATTCTTTGGAGCG-3′, 3′ primer, 5′-CAATCATGAAGGTGAGCAGG-3′; MBP: 5′ primer, 5′-TACCTGGCCACAGCAAGTAC-3′, 3′ primer, 5′-GTCACAATGTTCTTGAAG-3′; MAG: 5′ primer, 5′-TGCTCACCAGCATCCTCACG-3′, 3′ primer, 5′-AGCAGCCTCCTCTCAGATCC-3′; Omgp: 5′ primer, 5′-GCAGCAGCTGCAACTCTAAC 3′, 3′ primer, 5′-GAAGCATTTACTTTCCAAGCA-3′; MOG: 5′ primer, 5′-CCAAGAGGAGGCAGCAATGG-3′, 3′ primer, 5′-GTTGTAGCAGATGATCAAGG-3′; CGT: 5′ primer, 5′-GAAATTCACAAGGATCAACC 3′, 3′ primer, 5′-GTC-CATTAACTGTGCTATGC-3′; Cyclophilin: 5′ primer, 5′-ACACGCCATAATGGCACTGG-3′, 3′ primer, 5′-TGGTGATCTTCTTGCTGGTC; HPRT: 5′ primer, 5′-TGAACGTCTTGCTCGAGATG-3′, 3′ primer, 5′-GTTGAGAGATCATCTCCACC-3′; GAPDH: 5′ primer, 5′-GAGCTGAACGGGAAGCTCAC-3′, 3′ primer, 5′-CACCACCCTGTTGCTGTAGC-3′.

Isolation of Myelin and Protein Analysis

Myelin from 42-day-old mouse brain was purified by sucrose density gradient centrifugation following established procedures (Norton and Poduslo, 1973). Aliquots were separated on 15% SDS-PAGE. Polyacrylamide gels were silver- or Coomassie-stained. Western blot analysis was performed with SuperSignalSubstrate (Pierce, Rockford, IL) using a polyclonal anti-PLP antibody (whole protein) generated in our laboratory.

Light and Electron Microscopy

Twenty-day, 36-day, 5-month, and 14-month-old anesthetized wild-type and homozygous $dm20_{only}$ mice were perfused with 6% glutaraldehyde via the left cardiac ventricle. The optic nerve and cervical segments of the spinal cord were isolated, postfixed in 1% phosphate-buffered OsO_4 in 0.1 M sucrose, and embedded in Epon 812. The semithin sections were stained with toluidine/pyronin. Ultrathin sections were contrasted with uranyl acetate and lead citrate and examined as described previously (Büssow, 1978). The sections were compared to sections of 3- and 14-month-old *plp*−/− mutants.

RESULTS

$dm20_{only}$ Replacement Vector and Characterization of Recombinant ES Cell Clones

The expression of PLP was eliminated by the deletion of the distal 105 bp of exon III to obtain the

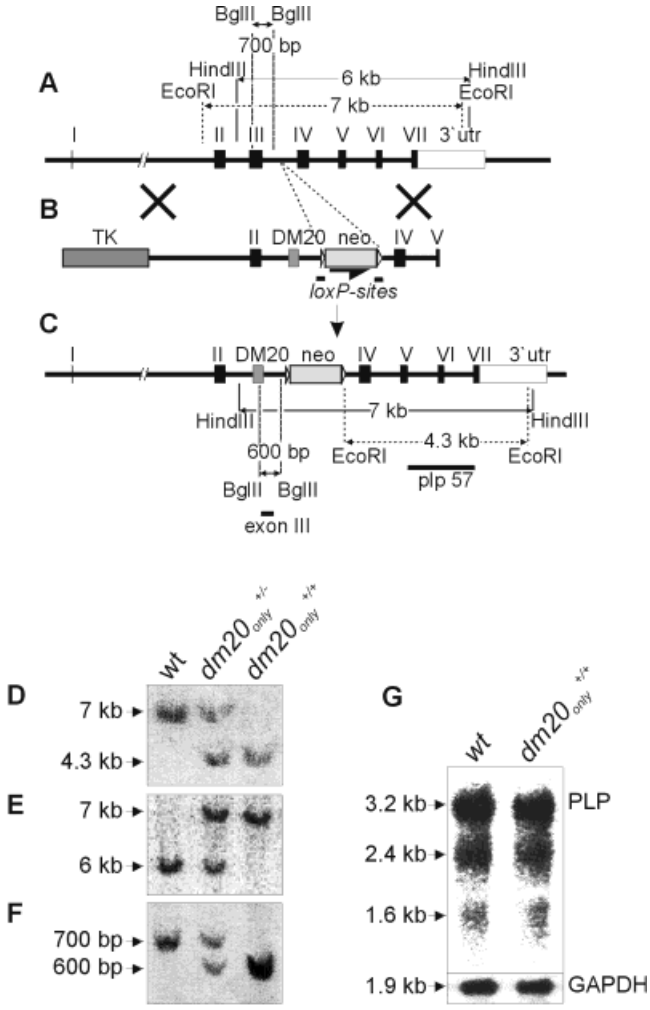

Fig. 1. Targeted mutagenesis of the mouse *plp* locus. **A:** Map of the endogenous *PLP* gene. **B:** Targeting construct. **C:** Expected replacement event after homologous recombination. Exons are represented by closed boxes. The neomycin resistance gene (*neo*) was inserted in intron III in sense orientation. The 3′ region of exon VII encodes the 3′ untranslated region of normal PLP mRNA (open box). The location of the hybridization probes *exon III* and *plp57* are shown (black bars). The arrows indicate the characteristic *Eco*RI, *Hind*III, and *Bgl*II fragments in wild-type and recombinant loci. **D** and **E:** Southern blot analysis of tail DNA from wild-type (*wt*), heterozygous $dm20_{only}$ and hemizygous $dm20_{only}$ mice. Tail DNA was digested with *Eco*RI (D) and *Hind*III (E) and hybridized with the probe *plp57*. The *Eco*RI digestion leads to a 7 kb fragment in wild-type and a 4.3 kb fragment in mutant mice. The *Hind*III digestion yielded a 7 kb fragment in mutant and a 6 kb fragment in wild-type mice. To verify the DM20-specific deletion of 105 bp tail, DNA was digested with *Bgl*II and hybridized with the probe *exon III* (**F**). Wild-type alleles cut with *Bgl*II generated a band of 700 bp, mutated alleles yielded a band of 600 bp. **G:** Northern blot analysis of total RNA isolated from brains of 20-day-old $dm20_{only}$ and wild-type mice. RNA was probed with a PLP cDNA fragment and as a control with a GAPDH cDNA probe.

PLP-deficient $dm20_{only}$ construct for targeting the *plp* locus by homologous recombination. Figure 1A resembles the $dm20_{only}$ construct that we used for electroporation of mouse embryonic stem cells CJ7 (ES) cells. *Eco*RI and *Hind*III restriction analyses revealed the 7 kb *Hind*III fragment diagnostic for the wt and the 4.3 kb *Eco*RI for the homologous recombination event (Fig. 1A–C). A *Bgl*II restriction site in the *dm20* and *wt* exon

III was used to verify the deletion of the PLP-specific sequence. Due to the 105 bp deletion, a 600 bp diagnostic fragment in contrast to the wt 700 bp fragment appeared in Southern blot analysis with an internal exon III probe (data not shown). Two CJ7 ES cell clones that showed the correct homologous recombination were selected for the generation of the PLP-deficient $dm20_{only}$ mice.

Generation and Characterization of PLP-Deficient $dm20_{only}$ Mice

$dm20_{only}$ ES cells were injected into blastocysts from inbred C57/B6 mice following standard procedures. Figure 1D–F outlines the genotyping of the hetero- and hemizygous siblings. The restriction and hybridization strategy outlined for the ES cell analysis was applied. These analytical data clearly proved that we had generated a $dm20_{only}$ homozygous mouse line.

$dm20_{only}$ Mice Express Three plp-Specific mRNAs

The impact of the deletion in exon III on the *dm20* expression was first studied by Northern blot hybridization analysis. Total RNA from brains of 20-day-old hetero- and hemizygous $dm20_{only}$ mice contained the three specific mRNAs of 1.6, 2.4, and 3.2 kb indiscriminately in size and expression level from the *wt* pattern. The splicing of the exclusively expressed *dm20* primary transcript is unimpaired (Fig. 1G).

dm20 Expression in Myelinating and Nonmyelinating Tissue of wt and $dm20_{only}$ Mice

Oligodendrocytes reach maximal specific expression of genes encoding myelin-specific proteins around p15 and p25. We measured the expression kinetics of *plp* and *dm20* transcripts during the myelination period by quantitative RT-PCR in *wt* and $dm20_{only}$ brain. The expression of *dm20* transcripts in the $dm20_{only}$ mouse mutant is comparable to *wt*, indicating that the PLP promoter activity is not affected by the targeted mutation (Fig. 2A). An early appearance of *plp* transcripts has been observed in fetal bovine hemispheres (Van Dorsselaer et al., 1987; Schindler et al., 1990) and in the developing *wt* mouse (Timsit et al., 1992; Peyron et al., 1997). Our results confirm these observations. DM20 mRNA has been recognized as a marker of oligodendroglial precursor cells emerging from the germinative neuroepithelium in the ventral neural tube; however, no DM20 translation product has been found (Timsit et al., 1995).

Ectopic expression of the oligodendrocyte-specific *plp* gene in heart and thymus of the $dm20_{only}$ mouse is noteworthy to mention. The expression of PLP and DM20 splice products in thymus is detected around p17

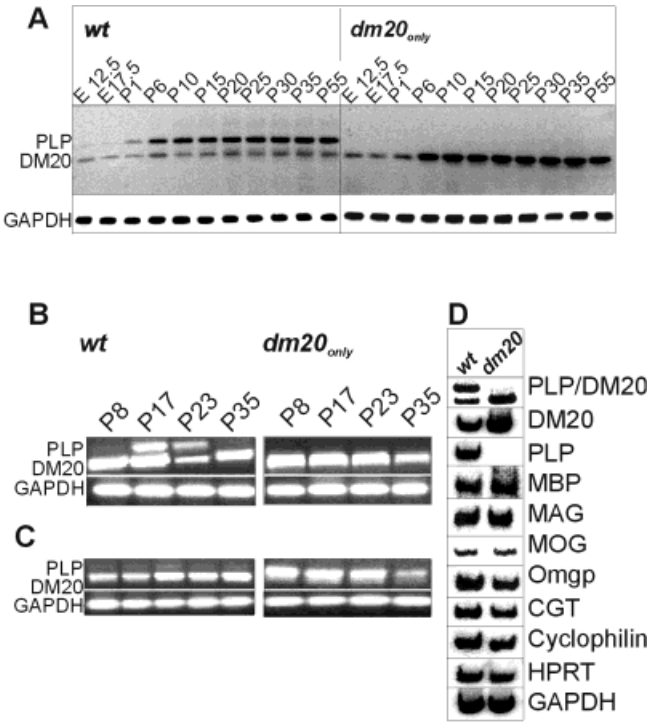

Fig. 2. **A:** RT-PCR analysis of PLP mRNA in *wild-type* (*wt*) and homozygous ($dm20_{only}$) mice. PCR was performed on cDNA derived from total brain RNA isolated from E 12.5-, E17.5-, 1-, 6-, 10-, 15-, 20-, 25-, 30-, 35-, and 55-day-old mice. The primers were derived from exon II and IV. **B** and **C:** Developmental expression of PLP and DM20 in thymus (B) and heart (C). **D:** Quantitative RT-PCR analysis of myelin-specific genes normalized to the expression of GAPDH, Cyclophilin and HPRT. The internal endogenous standard procedure was applied in duplicate. We measured the $[^{32}P]$-dCTP activity incorporated into the 700 bp PCR fragment obtained with the primers neo and IVa. The activities were compared with those of housekeeping genes GAPDH, cyclophilin, and HPRT (hypoxanthine phosphoribosyl-transferase) in the linear range of the PCR kinetics between 17 and 23 cycles.

to p23, whereas only DM20 transcripts are observed before and after the myelination period. As expected, thymus of $dm20_{only}$ mice only expresses the DM20 transcript between p8 and p35 persisting over the myelination period (Fig. 2B).

In agreement with earlier reports (Campagnoni et al., 1992; Nadon et al., 1997), predominantly *dm20* transcripts are amplified from RNA of *wt* heart between p8 and p35 at equal yield; however, in $dm20_{only}$ mice, maximal *plp* promoter activity around p20 enhances DM20 expression more than twofold (Fig. 2C).

Regulation of Expression of Other Myelin Genes Is Not Affected by PLP-Specific Deletion

Total brain mRNA of myelinating (p20) mice was analyzed by quantitative RT-PCR to determine the transcriptional regulation of the *PLP* gene together with some dominant oligodendrocyte and myelin-specific genes (Fig. 2D). Amplified PCR DNA fragments of the genes indicated in Figure 2 and the respective housekeeping genes were separated by polyacrylamide

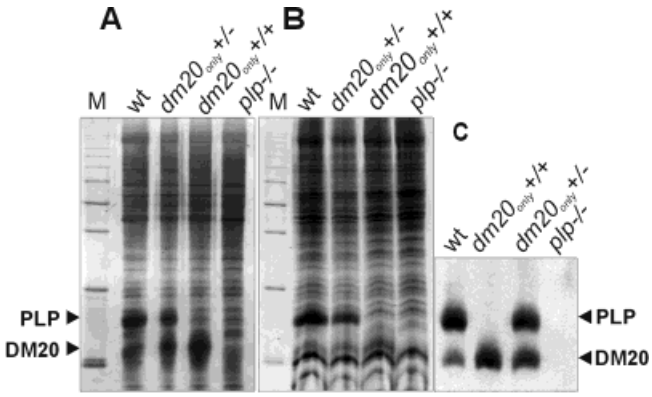

Fig. 3. **A** and **B:** Silver- and Coomassie-stained SDS-PAGE (15%) protein analysis of CNS myelin proteins. **C:** Western blot analysis of myelin proteins from $dm20_{only}$ and wild-type mice using a polyclonal anti-PLP antibody (whole protein) generated in our laboratory.

gel electrophoresis and quantified with a Phosphor Imager. The expression of *mbp*, *mag*, *mog*, *omgp*, and *cgt* was compared with that of *plp*. As expected, the PLP-specific transcripts are missing in the $dm20_{only}$ mutant. The *dm20* transcription equals the sum of the PLP and DM20 transcripts of the wt. The products of the other genes studied remain unaltered (Fig. 2D).

$dm20_{only}$ Mice Exhibit a wt-Like Myelin Protein Pattern

Myelin from 2-month-old *wt*, hetero- and homozygous mouse brains was isolated by sucrose gradient centrifugation (Norton and Poduslo, 1973). Myelin mass recovery from the three genotypes wt, dm20+/−, and dm20+/+ was identical. The myelin protein pattern was analyzed by SDS-PAGE (15%) analysis. The complete absence of the PLP isoform confirms the specific and only expression of the DM20 isoform on the RNA level in the $dm20_{only}$ mouse: PLP-specific protein was absent in the otherwise unchanged protein pattern of the $dm20_{only}$ mutant. The signal intensity of the DM20 isoform in the homozygous $dm20_{only}$ brain was equal to the sum of the PLP isoforms in the heterozygous mouse and missing in the *plp*−/− mouse brain as shown in silver- and Coomassie-stained gels and in the Western blot analysis (Fig. 3).

$dm20_{only}$ Oligodendrocytes Enwrap CNS Axons With Compact Myelin That Degenerates With Aging

We studied the myelinated axons of the optic nerve of $dm20_{only}$ and *plp*−/− mutants mice of 3 and 5 month of age by electron microscopy. Ultrastructurally, axons of $dm20_{only}$ CNS are ensheathed by normal myelin membranes as shown in cross-sections of $dm20_{only}$ and *wt* optic nerve. Their difference to *plp*−/− myelin is demonstrated in Figure 4. Unlike the hypomyelinating *plp*−/− mutant, small-diameter axons of the $dm20_{only}$ mouse are myelinated like wt axons. In $dm20_{only}$ and *plp*−/− mutants, myelin sheaths with remaining oligodendrocyte cytoplasm are detectable (indicated by arrows in Figure 5A and B). Axonal spheroids as shown in *plp*−/− sections (asterisk in Fig. 5B) are not detectable in sections of $dm20_{only}$ mice but rarely degenerating nerve fibers (asterisk in Fig. 5C). Oligodendrocytes of $dm20_{only}$ mice also produce redundant myelin (Figs. 5C and 6).

The periodicity of the tightly compacted multilayer myelin membrane of *wt* and $dm20_{only}$ mice is comparable. We have statistically validated the periodicities of the myelin sheaths of axons of $dm20_{only}$ mutants in comparison with *wt* myelin (Fig. 7, Table 1). The ultrastructure differs distinctly from the PLP-deficient mouse, lacking both PLP isoforms and missing their adhesive properties on the outer surface of the membrane. Unlike *wt* CNS, the $dm20_{only}$ optic nerve shows a small number of degenerating myelin sheaths.

DISCUSSION

In previous studies, we have generated a homozygous mouse line devoid of the 30 kDa PLP and its 26 kDa isoform DM20 to determine the function of these main integral membrane constituents of the myelin sheath of CNS axons. Here we address the question regarding the function of the evolutionary ancestral DM20 isoform by deleting the expression of the PLP isoform. The terminal 3′ 105 bp exon III in our targeting construct, encoding the PLP-specific sequence, has been truncated. The selection marker (*neo* gene) resided in intron 3 in sense orientation. In the resulting homozygous mouse line, transcription yielded equivalent amounts in comparison to *wt* controls, in contrast to the neo-cassette in intron III in antisense orientation, which led to a complete suppression of PLP transcription products (Boison and Stoffel, 1994). In agreement with these results, the sense-oriented *neo* gene in a corresponding neo-sense mouse reduced the transcription product of the plp isoform by 50%–60% but not of the DM20 isoform (data not shown).

The translation of the mRNA in the myelinating mice yielded only the isoform DM20. The genetic and biochemical analysis proved that we had generated the $dm20_{only}$ mouse line deficient in PLP. Different functions have been assigned to PLP and DM20 in myelin structure and oligodendrocyte development (Nadon and West, 1998). The function(s) of the cytoplasmic loop harboring the PLP-specific amino acid still remains elusive.

Different from our strategy, by which the PLP-specific 105 bp of exon III of the targeting construct were deleted for the generation of the $dm20_{only}$ mouse mutant, another mouse line expressing only DM20 has been generated (Stecca et al., 2000): the splice donor site of intron III has been mutated in *E. coli* and a

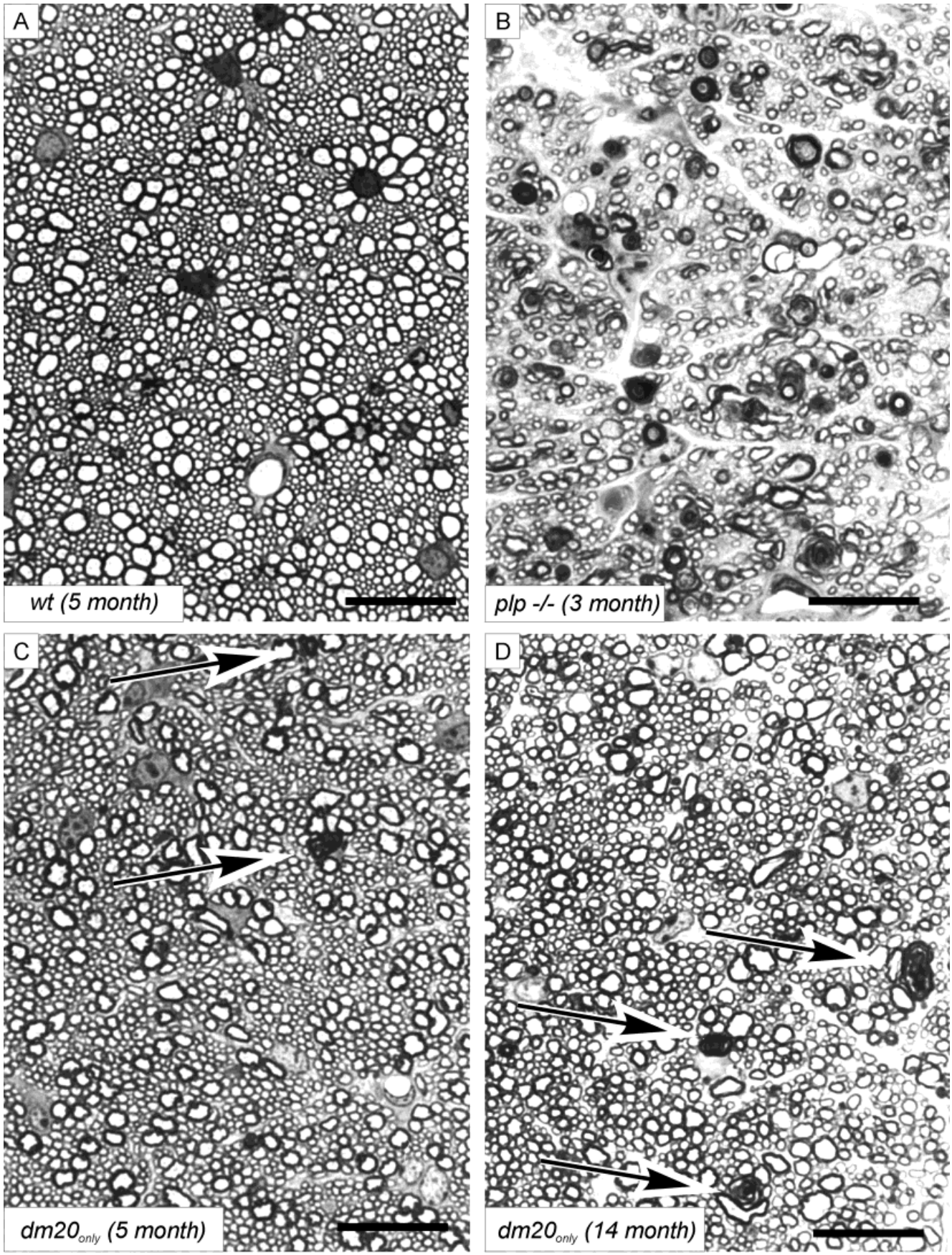

Fig. 4. Semithin cross-sections through the optic nerves of 5 month old wild-type (**A**), 3-month-old *plp*−/− (**B**), 5- and 14-month-old $dm20_{only}$ (**C** and **D**). The comparison of the $dm20_{only}$ sections (C and D) shows an increasing ratio of degenerating myelin sheaths. In contrast to the homozygous *plp*−/− mutant, no hypomyelination is detectable in the $dm20_{only}$ sections (B and D). Scale bar = 16 μm.

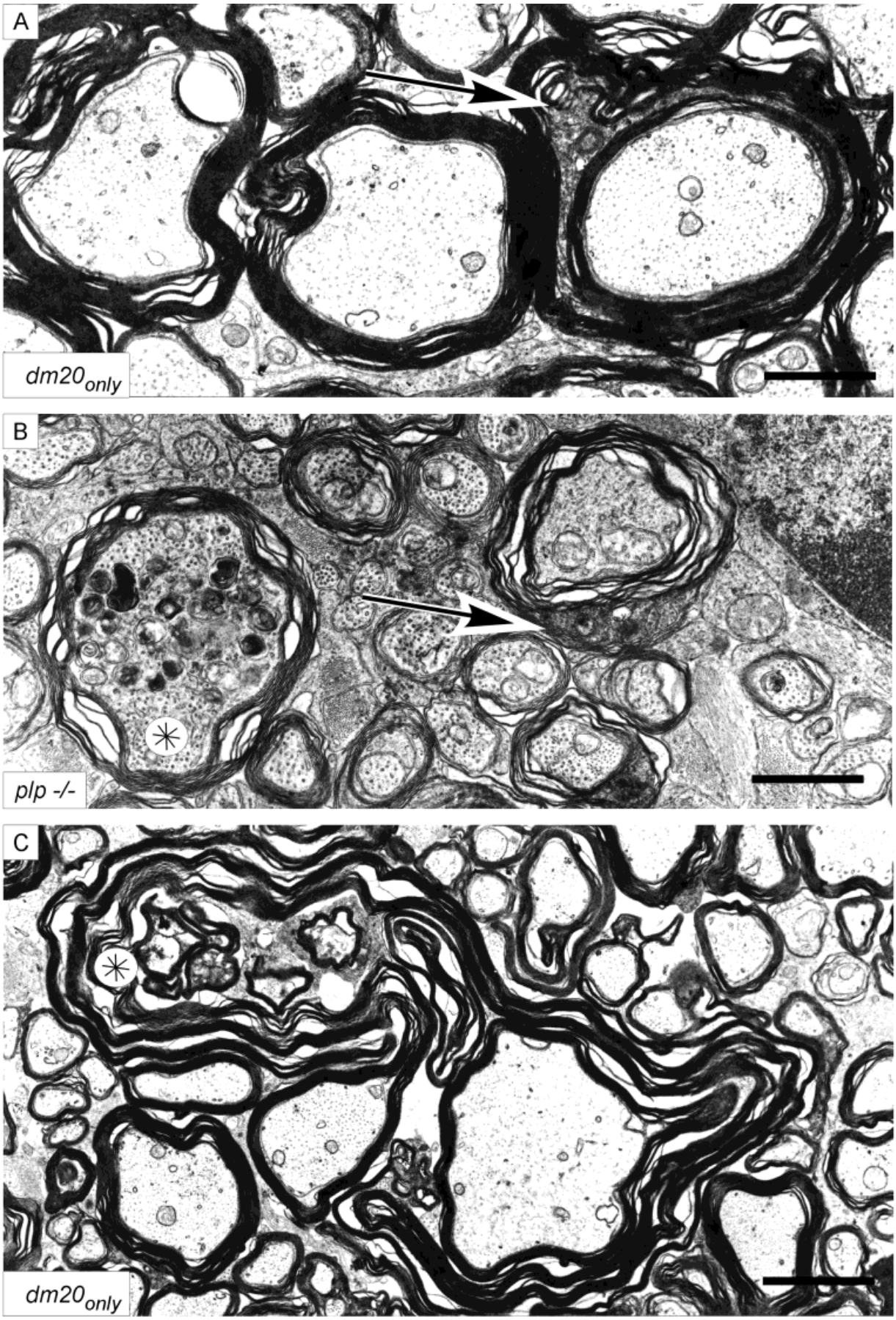

Fig. 5. **A** versus **B:** In contrast to *plp*−/− mutants, the myelin sheaths of $dm20_{only}$ are compacted. Sheaths of both *plp*−/− and $dm20_{only}$ mutants contain oligodendrocyte cytoplasm in compact myelin (A, B, arrows) depicting the beginning of degeneration of myelin sheaths. Scale bar = 2.4 μm. A progressive stage of degeneration is seen in **C** (asterisk), where electron micrographs showing redundant myelin and a degenerating nerve fiber in $dm20_{only}$ mutants (asterisk). Scale bar = 1.2 μm. Axonal spheroids (in *plp*−/− sections, B, asterisk) are not detectable in $dm20_{only}$ mutants.

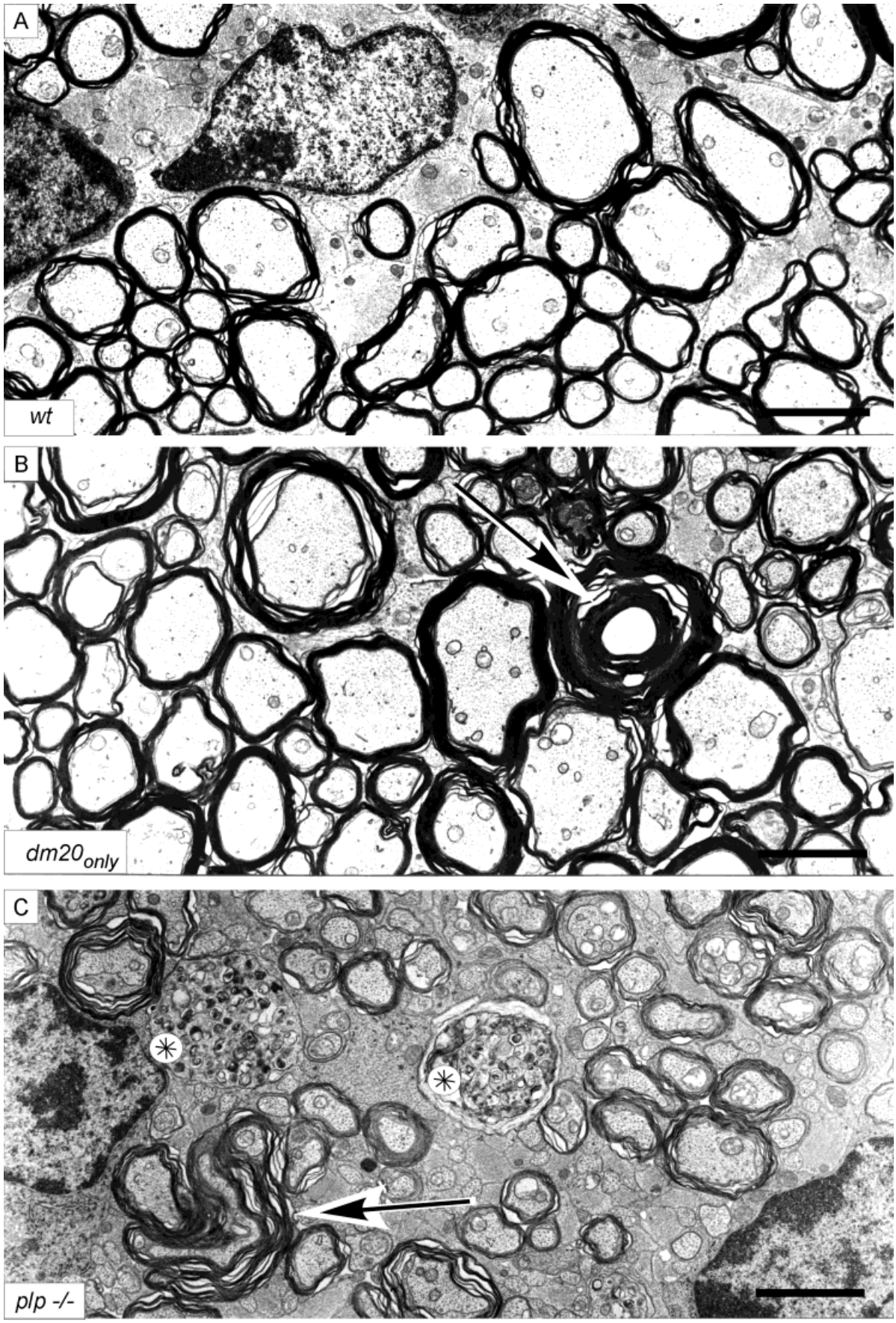

Fig. 6. Low-power electron micrographs of cross-sections through the optic nerve. **A:** Wild-type (5 month). **B:** $dm20_{only}$ (5 month). **C:** *plp*−/− (3 month). Only in *plp*−/− mice axonal spheroids and the abnormal accumulation of organelles in the paranodal space respectively are observed (C, asterisk) and not in $dm20_{only}$ mutants. All axons of wild-type and $dm20_{only}$ mutants are myelinated and show compact ensheathments. In addition, redundant myelin (arrows) is visible in $dm20_{only}$ and *plp*−/− mutants. Scale bar = 2.4 μm.

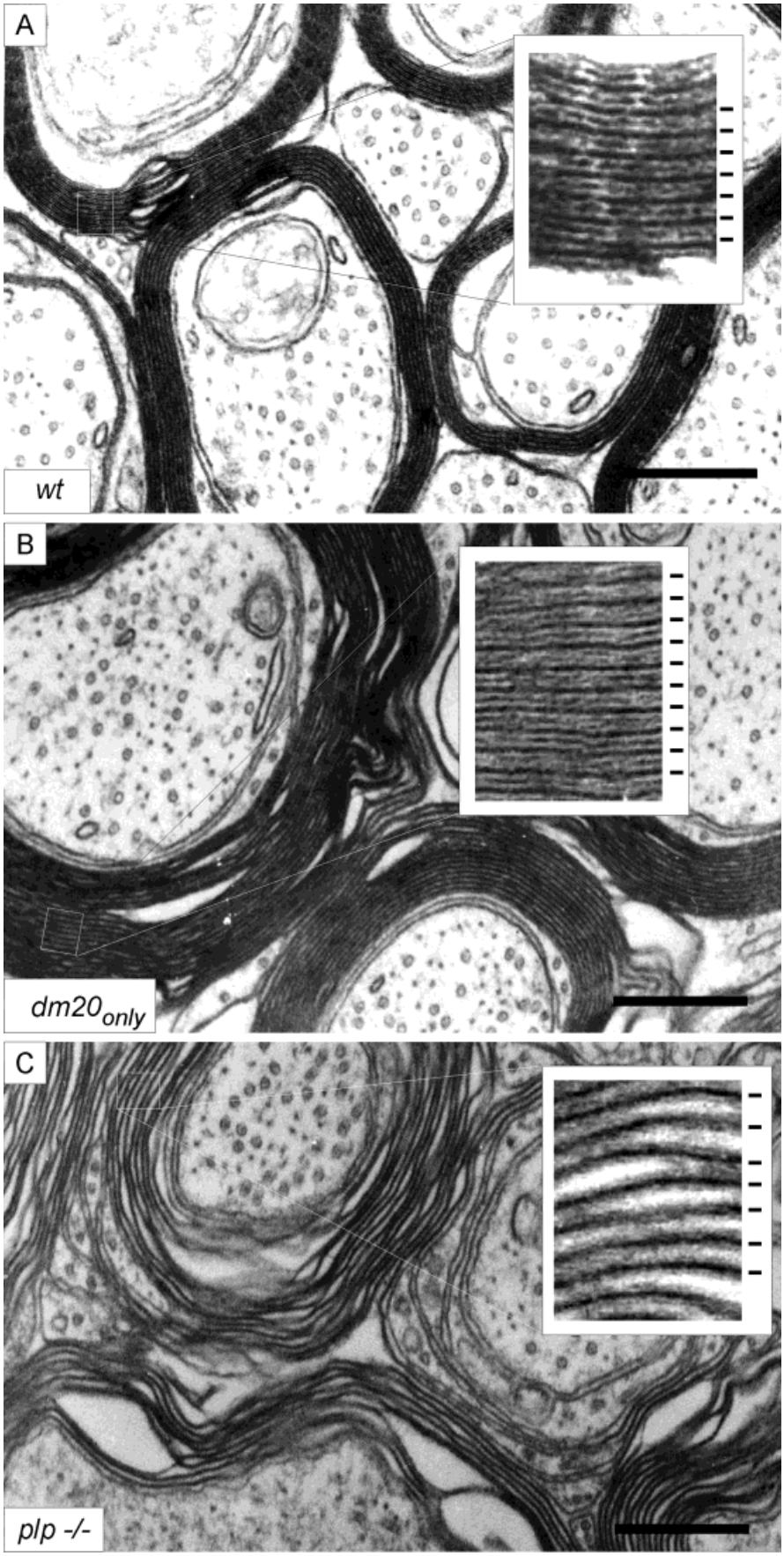

Fig. 7. **A** and **B:** Electron micrograph (optic nerve) showing normal periodicity of sections of 14 months old *wild-type* and $dm20_{only}$ mutants. **C:** Decompacted myelin sheaths of *plp*−/− mutants. Fixation procedures were identical for all samples (6% glutaraldehyde). Scale bar = 0.36 μm.

TABLE 1. Periodicities of wt *and* dm20$_{only}$ *CNS myelin**

Genotype	Sections analyzed	Number of measured periodicities	Periodicity (nm)
dm20$_{only}$	23	618	14.08 ± 0.84
Wild-type	14	435	14.05 ± 0.63

*Results represent mean values ± SEM.

floxed neo-cassette introduced into a loxP site in intron III by transient Cre-mediated recombination. ES cells homologously recombined with this construct yielded homozygous mice, embryos of which received a Cre-recombinase encoding vector by pronuclear injection before reimplantation into pseudopregnant mice.

We expected from the *dm20*$_{only}$ mouse mutant insight into specific functions of DM20, e.g., in the assembly and maintenance of the CNS myelin structure and its role in the development of oligodendrocytes and in protein transport during myelination. The findings and the conclusions drawn from the two mouse models generated by two very different strategies are partly in accordance but differ distinctly in others.

The synergism of both isoforms PLP and DM20 for the maturation of oligodendrocytes has been deduced from rescue experiments (Nadon and West, 1998). Intracellular transport of PLP to the plasma membrane of heterologously expressing HeLA cells is supposed to require both PLP and DM20 isoforms (Gow et al., 1994). DM20 overexpressing transgenic mouse lines show age- and copy number–dependent demyelination (Johnson et al., 1995). The genetic experiments and ultrastructural analysis described here and the normal oligodendrocyte development in the *plp*−/− mouse line, deficient in PLP as well as in DM20 (Boison and Stoffel, 1994), make it highly unlikely that DM20 plays an essential role in the differentiation and compartmentalization of oligodendrocytes in brain.

However, at age 3 to 5 months in myelin sheaths of a few axons of *dm20*$_{only}$ mice, cytoplasmic inclusions accumulate within compacted myelin. Cytoplasmic inclusion structures were also observed in DM20 overexpressing mice (Mastronardi et al., 1993) and in null allelic PMP22 (Adlkofer et al., 1997), NCAM (Carenini et al., 1997), and MAG mice (Yin et al., 1998). These cytoplasmic pockets have been interpreted as onset of myelin and/or axonal degeneration, structures never observed in normal *wt* white matter.

Different from the observation reported by Stecca et al. (2000) and unlike the aging *plp*−/− mouse (Boison and Stoffel, 1994), our *dm20*$_{only}$ mouse lacks the numerous axonal swellings and axon degenerations. In agreement with a rescue experiment crossing a DM20-transgenic mouse line to the *plp*−/− mouse (Griffiths et al., 1998), we were unable to detect a diffuse gliosis. With growing age, a punctuated dissociation of the compact myelin layers at their cytosolic surfaces (MDL) leads to the formation of cytoplasmic pockets, and the rare appearance of redundant myelin and degeneration of oligodendrocytes in the aging brain (> 5 months) of *dm20*$_{only}$ mice hint at a minor dysregulation of the synthesis of myelin constituents by oligodendrocytes during myelination. However, these changes do not result in a pathological phenotype even after almost 2 years.

What are the consequences of the missing PLP-specific sequence in the large cytosolic loop for the structure (morphology) and maintenance of the compacted myelin membrane? Does the PLP-specific sequence influence the topology or the dimensions of the periodicity?

In order to elucidate possible morphological alterations of the compact myelin membrane system due to the missing PLP-specific sequence of the large cytosolic loop, we compared the periodicity of the myelin sheath of axons of optic nerve of *wt* and *dm20*$_{only}$ mice to answer the question whether DM20 can structurally substitute for PLP. Figure 7 paradigmatically displays cross-sections of wt and mutant optic nerve, fixed and stained under identical conditions. More than 500 periodicities of segments of the multiple *wt* and 400 *dm20*$_{only}$ myelin membrane layers of mice 5–6 months of age were measured for statistical evaluation (Table 1). These results underline that the periodicity of the CNS myelin sheaths with only DM20 (*dm20*$_{only}$) or both isoforms PLP and DM20 (*wt*) as integral membrane proteins are identical. An impact of the cytosolic PLP-specific sequence missing in DM20 on the periodicity cannot be verified morphologically. We conclude that DM20 can fully substitute PLP in the CNS myelin membrane regarding myelin periodicity and compaction.

Our measurements are at variance with the report by Stecca et al. (2000), in which a 20% expanded periodicity of the cerebellum myelin of DM20 expressing mice has been reported. This increase has been attributed to a broadened intraperiod dense line due to a shift of the third TMD toward the external surface. A pivotal role of the 35 amino acid PLP-specific sequence for a normal myelin periodicity and long-term stability of the myelin sheath and the axon-glia interaction has been concluded. Different from these results, we observed an overall normal stability of the myelin membrane in p20, 3-, 6-, and 12-month-old *dm20*$_{only}$ mice unlike the massive dissociation of the individual myelin layers in the *plp*−/− mouse. The periodicity of optic nerve myelin of the *dm20*$_{only}$ and *wt* mouse is identical (about 14 nm), in agreement with X-ray diffraction studies in fresh CNS nerve (about 12 nm) (Kirschner and Blaurock, 1991). The identical spacing in wt and mutant myelin under our fixation conditions (perfusion with 6% glutaraldehyde) demonstrates that the substitution of PLP by DM20 causes no morphologically visible structural rearrangement. DM20 therefore can substitute for the lack of the PLP isoform and maintain the overall periodicity of the main dense line (MDL) and intermediate dense line (IDL) of CNS myelin.

Early ectopic expression in heart and thymus has been observed. Intrathymic expression of *plp* is not restricted to the DM20 isoform. Around p15–p25, it is

associated transiently with the strongly expressed PLP splice variant. This might explain the T-cell tolerance to all epitopes of PLP in EAE-resistant C57BL/6 mice reported recently (Klein et al., 2000). In heart, DM20 is much stronger-expressed than the PLP isoform that lasted beyond the myelination period. This ectopic expression of the oligodendrocyte-specific PLP and DM20 mRNAs might be caused either by the strong PLP promoter activity or the leakiness of unbalanced silencer activity for time- and cell-specific regulated expression (Berndt et al., 1992; Armstrong et al., 1995; Pott et al., 1995; Kim et al., 1997).

A different structure-function aspect of the complete substitution of the PLP isoform by DM20 in the plasma membrane processes of the oligodendrocyte might be of importance. PLP contains up to six long-chain fatty acyl residues linked to cysteine residues by thioester bonds within hydrophilic loop 1 (cys 5, 6, and 9) and loop 3 (cys 108, 138, and 140). DM20 is missing the two acylated cysteines 138 and 140 of the PLP-specific sequence.

The number and the positions of cysteine residues, including the two disulfide bonds in the large extracytoplasmic hydrophilic loop 4, for posttranslational palmitoylation and disulfide formation are phylogenetically conserved between amphibians, chicken, and human except cys108, which is substituted by met in amphibians.

This suggests an essential role for these posttranslational modifications for PLP structure and function (Bizzozero and Good, 1991; Schließ and Stoffel, 1991; Bizzozero et al., 1999; Messier and Bizzozero, 2000), which is not understood. Fatty acyl groups are transferred nonenzymatically and/or enzymatically to PLP cysteine residues and released by a palmitoyl-protein-thioesterase in a dynamic process (Bizzozero et al., 1987), which remains elusive.

The covalently linked long-chain fatty acyl chains on the cytosolic domains (N-terminus, loop 3) have two choices to interact with the hydrophobic environment of adjacent lipid bilayers. Fatty acyl chains might intercalate into the same bilayer leaflet (cys5, cys6, and cys9) or into the opposite leaflet (cys108, cys138, and cys140). This would further stabilize the adhesion of the adjacent cytosolic surfaces in the MDL. Figure 8 schematically depicts the suggested topology of tetraspan DM20 (Weimbs and Stoffel, 1994).

Two of the six acylation sites (cys138 and cys140) are located within the PLP-specific sequence of the third cytosolic loop, missing in DM20. We hypothesize that the lack of the two acyl groups in DM20 might weaken the strong hydrophobic adhesive forces in the cytosol leading to the formation of cytoplasmic pockets in myelin of the $dm20_{\text{only}}$ mouse described in Figure 6. Further genetic experiments are necessary to prove the hypothetical role of PLP palmitoylation for the stability and maintenance of the myelin membrane.

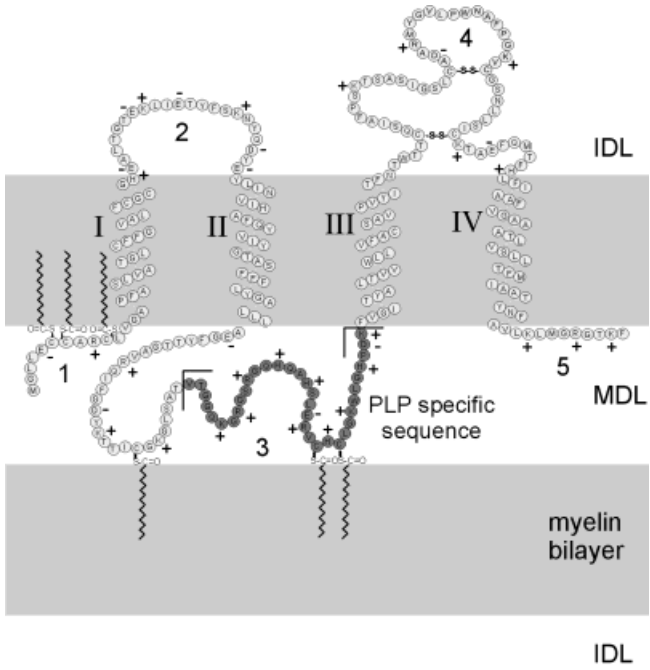

Fig. 8. Proposed PLP topology with fatty acyl intercalation into the lipid bilayer of plasma membrane processes (myelin sheath). The region deleted in DM20 is indicated.

REFERENCES

Adlkofer K, Frei R, Neuberg DH, Zielasek J, Toyka KV, Suter U. 1997. Heterozygous peripheral myelin protein 22-deficient mice are affected by a progressive demyelinating tomaculous neuropathy. J Neurosci 17:4662–4671.

Armstrong RC, Kim JG, Hudson LD. 1995. Expression of myelin transcription factor I (MyTI), a "zinc-finger" DNA-binding protein, in developing oligodendrocytes. Glia 14:303–321.

Berndt JA, Kim JG, Hudson LD. 1992. Identification of cis-regulatory elements in the myelin proteolipid protein (PLP) gene. J Biol Chem 267:14730–14737.

Bizzozero O, McGarry J, Lees M. 1987. Autoacylation of myelin proteolipid protein with acyl coenzyme A. J Biol Chem 262:13550–13557.

Bizzozero OA, Good LK. 1991. Rapid metabolism of fatty acids covalently bound to myelin proteolipid protein. J Biol Chem 266: 17092–17098.

Bizzozero OA, Sanchez P, Tetzloff SU. 1999. Effect of ATP depletion on the palmitoylation of myelin proteolipid protein in young and adult rats. J Neurochem 72:2610–2616.

Boison D, Stoffel W. 1989. Myelin-deficient rat: a point mutation in exon III (A-C, Thr75-Pro) of the myelin proteolipid protein causes dysmyelination and oligodendrocyte death. EMBO J 8:3295–3302.

Boison D, Stoffel W. 1994. Disruption of the compacted myelin sheath of axons of the central nervous system in proteolipid protein-deficient mice. Proc Natl Acad Sci USA 91:11709–11713.

Boison D, Büssow H, D'Urso D, Müller H-W, Stoffel W. 1995. Adhesive properties of proteolipid protein are responsible for the compaction of CNS myelin sheaths. J Neurosc 15:5502–5513.

Bradley A, Evans M, Kaufman M, Robertson E. 1984. Formation of germ-line chimaeras from embryo-derived teratocarcinoma cell lines. Nature 309:255–256.

Büssow H. 1978. Schwann cell myelin ensheathing C.N.S. axons in the nerve fibre layer of the cat retina. J Neurocytol 7:207–214.

Campagnoni CW, Garbay B, Micevych P, Pribyl T, Kampf K, Handley VW, Campagnoni AT. 1992. DM20 mRNA splice product of the myelin proteolipid protein gene is expressed in the murine heart. J Neurosci Res 33:148–155.

Carenini S, Montag D, Cremer H, Schachner M, Martini R. 1997. Absence of the myelin-associated glycoprotein (MAG) and the neural cell adhesion molecule (N-CAM) interferes with the maintenance, but not with the formation of peripheral myelin. Cell Tissue Res 287:3–9.

Chomczynski P, Sacchi N. 1987. Single-step method of RNA isolation by acid guanidinium thiocyanate-phenol-chloroform extraction. Anal Biochem 162:156–159.

Diehl H-J, Schaich M, Budzinski R-M, Stoffel W. 1986. Individual exons encode the integral membrane domains of human myelin proteolipid protein. Proc Natl Acad Sci USA 83:9807–9811.

Gow A, Friedrich VL Jr, Lazzarini RA. 1994. Many naturally occurring mutations of myelin proteolipid protein impair its intracellular transport. J Neurosci Res 37:574–583.

Griffiths I, Klugmann M, Anderson T, Yool D, Thomson C, Schwab MH, Schneider A, Zimmermann F, McCulloch M, Nadon N, Nave KA. 1998. Axonal swellings and degeneration in mice lacking the major proteolipid of myelin. Science 280:1610–1613.

Johnson RS, Roder JC, Riordan JR. 1995. Over-expression of the DM-20 myelin proteolipid causes central nervous system demyelination in transgenic mice. J Neurochem 64:967–976.

Kim JG, Armstrong RC, Agoston D, Robinsky A, Wiese C, Nagle J, Hudson LD. 1997. Myelin transcription factor 1 (Myt1) of the oligodendrocyte lineage, along with a closely related CCHC zinc finger, is expressed in developing neurons in the mammalian central nervous system. J Neurosci Res 50:272–290.

Kirschner DA, Blaurock AE. 1991. Organization, phylogenetic variations and dynamic transitions of myelin. In: Martenson RE, editor. Myelin: biology and chemistry. Boca raton, Fl: CRC Press. p 413–448.

Kitagawa K, Sinoway MP, Yang C, Gould RM, Colman DR. 1993. A proteolipid protein family: expression in sharks and rays and possible evolution from an ancestral gene encoding a pore-forming polypeptide. Neuron 11:433–448.

Klein L, Klugmann M, Nave KA, Tuohy VK, Kyewski B. 2000. Shaping of the autoreactive T-cell repertoire by a splice variant of self protein expressed in thymic epithelial cells. Nat Med 6:56–61.

Klugmann M, Schwab MH, Puhlhofer A, Schneider A, Zimmermann F, Griffiths IR, Nave KA. 1997. Assembly of CNS myelin in the absence of proteolipid protein. Neuron 18:59–70.

Mastronardi FG, Ackerley CA, Arsenault L, Roots BI, Moscarello MA. 1993. Demyelination in a transgenic mouse: a model for multiple sclerosis. J Neurosci Res 36:315–324.

Messier AM, Bizzozero OA. 2000. Conserved fatty acid composition of proteolipid protein during brain development and in myelin subfractions. Neurochem Res 25:449–455.

Milner R, Lai C, Nave K, Lenoir D, Ogata J, Sutcliffe J. 1985. Nucleotide sequences of two mRNAs for rat brain myelin proteolipid protein. Cell 42:931–939.

Nadon NL, Miller S, Draeger K, Salvaggio M. 1997. Myelin proteolipid DM20: evidence for function independent of myelination. Int J Dev Neurosci 15:285–293.

Nadon NL, West M. 1998. Myelin proteolipid protein: function in myelin structure is distinct from its role in oligodendrocyte development. Dev Neurosci 20:533–539.

Nave K, Lai C, Bloom F, Milner R. 1986. Jimpy mutant mouse: a 74 base deletion in the mRNA for myelin proteolipid protein and evidence for a primary defect in RNA splicing. Proc Natl Acad Sci USA 83:9264–9268.

Nave K-A, Lai C, Bloom FE, Milner RJ. 1987. Splice site selection in the proteolipid protein (PLP) gene transcript and primary structure of the DM-20 protein of central nervous system myelin. Proc Natl Acad Sci USA 84:5665–5669.

Norton W, Poduslo S. 1973. Myelination in rat brain: method of myelin isolation. J Neurochem 21:749–757.

Peyron F, Timsit S, Thomas JL, Kagawa T, Ikenaka K, Zalc B. 1997. In situ expression of PLP/DM-20, MBP, and CNP during embryonic and postnatal development of the jimpy mutant and of transgenic mice overexpressing PLP. J Neurosci Res 50:190–201.

Popot JL, Dinh DP Dautigny A. 1991. Major myelin proteolipid:the 4α-ηελιξ τοπολογψ. J Membbr Biol 120:233–246.

Pott U, Thiesen HJ, Colello RJ, Schwab ME. 1995. A new Cys2/His2 zinc finger gene, rKr2, is expressed in differentiated rat oligodendrocytes and encodes a protein with a functional repressor domain. J Neurochem 65:1955–1966.

Redhead C, Popko B, Takahashi N, Shine H, Saavedra R, Sidman R, Hood L. 1987. Expression of a myelin basic protein gene in transgenic shiverer mice: correction of the dysmyelinating phenotype. Cell 48:703–712.

Schaich M, Budzinski R-M, Stoffel W. 1986. Cloned proteolipid protein and myelin basic protein cDNA. Biol Chem Hoppe-Seyler 367: 825–834.

Schindler P, Luu B, Sorokine O, Trifilieff E, Van Dorsselaer A. 1990. Developmental study of proteolipids in bovine brain: a novel proteolipid and DM-20 appear before proteolipid protein (PLP) during myelination. J Neurochem 55:2079–2085.

Schließ F, Stoffel W. 1991. Evolution of the myelin integral membrane proteins of the central nervous system. Biol Chem Hoppe-Seyler 372:865–874.

Stecca B, Southwood CM, Gragerov A, Kelley KA, Friedrich VL Jr, Gow A. 2000. The evolution of lipophilin genes from invertebrates to tetrapods: DM-20 cannot replace proteolipid protein in CNS myelin. J Neurosci 20:4002–4010.

Stoffel W, Hillen H, Schröder W, Deutzmann R. 1983. The primary structure of bovine brain myelin lipophilin (proteolipid apoprotein). Hoppe-Seyler's Z Physiol Chem 364:1455–1466.

Stoffel W, Giersiefen H, Hillen H, Schröder W, Tunggal B. 1985. Amino-acid sequence of human and bovine brain myelin proteolipid protein (lipophilin) is completely conserved. Biol Chem Hoppe-Seyler 366:627–635.

Stoffel W, Boison D, Büssow H. 1997. Functional analysis in vivo of the double mutant mouse deficient in both proteolipid protein and myelin basic protein in central nervous system. Cell Tissue Res 289:195–206.

Timsit S, Sinoway MP, Levy L, Allinquant B, Stempak J, Staugaitis SM, Colman DR. 1992. The DM20 protein of myelin: intracellular and surface expression patterns in transfectants. J Neurochem 58:1936–1942.

Timsit S, Martinez S, Allinquant B, Peyron F, Puelles L, Zalc B. 1995. Oligodendrocytes originate in a restricted zone of the embryonic ventral neural tube defined by DM-20 mRNA expression. J Neurosci 15:1012–1024.

Trifilieff E, Skalidis G, Helynck G, Lepage P, Sorokine O, Van Dorsselaer ABL. 1985. Structural data on the myelin proteolipid of apparent molecular weight 20 kDa (DM-20). CR Acad Sci III 300: 241–216.

Uschkureit T, Spörkel O, Stracke J, Büssow H, Stoffel W. 2000. Severe axonal degeneration in the proteolipid protein and myelin associated gylcoprotein deficient double (*plp*−/−mag−/−) and the plp−/−mbp−/−mag−/− triple mutant mouse. J Neurosci 20:5225–5233.

Van Dorsselaer A, Nebhi R, Sorokine O, Schindler P, Luu B. 1987. The DM-20 proteolipid is a major protein of the brain. It is synthetized in the fetus earlier than the major myelin proteolipid (PLP). CR Acad Sci III 305:555–560.

Weimbs T, Stoffel W. 1992. Proteolipid protein (PLP) of CNS myelin: positions of free, disulfide bonded, an fatty acid thioester-linked cysteine residues—implications for the membrane topology of PLP. Biochemistry 31:12289–12296.

Weimbs T, Stoffel W. 1994. Topology of CNS myelin proteolipid protein: evidence for the non-enzymatic glycosylation of extracytoplasmic domains in normal and diabetic animals. Biochemistry 33: 10408–10415.

Willard H, Riordan J. 1985. Assignment of the gene for myelin proteolipid protein to the X chromosome: implications for X-linked myelin disorders. Science 230:940–942.

Yin X, Crawford TO, Griffin JW, Tu P, Lee VM, Li C, Roder J, Trapp BD. 1998. Myelin-associated glycoprotein is a myelin signal that modulates the caliber of myelinated axons. J Neurosci 18:1953–1962.

Yool DA, Edgar JM, Montague P, Malcolm S. 2000. The proteolipid protein gene and myelin disorders in man and animal models. Hum Mol Genet 9:987–992.

Yoshida M, Colman DR. 1996. Parallel evolution and coexpression of the proteolipid proteins and protein zero in vertebrate myelin. Neuron 16:1115–1126.